Sains Malaysiana 52(1)(2023): 261-269
http://doi.org/10.17576/jsm-2023-5201-21

Optical Properties of Reduced Graphene Oxide-Coated Tellurite Glass Doped at Different Erbium Composition

(Sifat Optik Kaca Telurit Bersalut Graphene Oksida Terkurang Didop pada Komposisi Erbium Berbeza)

AZLINA YAHYA, MUHAMMAD NOORAZLAN ABD AZIS* & SURIANI ABU BAKAR

Physics Department, Faculty of Science and Mathematics, Universiti Pendidikan Sultan Idris, 35900 Tanjung Malim, Perak Darul Ridzuan, Malaysia

Received: 31 May 2022/Accepted: 11 October 2022

ABSTRACT

Graphene-based nanomaterials have significant potential to be used as coating materials for glass performance. In this work, reduced graphene oxide (rGO)-coated tellurite glass was synthesized via melt-quenching and low-cost spray coating techniques for improving the optical properties in the glassy matrix. The structural properties investigated using X-Ray Diffraction (XRD) confirmed the structural arrangement of an amorphous nature phase meanwhile, Scanning Electron Microscopy (SEM) analysis proved the morphological structure images of rGO onto the tellurite glass surface. The refractive index value of rGO-coated glass was found higher in the range of 2.402 - 2.775 due to the graphene-based effects. The optical bandgap energy value of rGO-coated glass was improved from 1.913 - 2.980 eV which correlated to the changes in rGO absorption characteristics. The Urbach energy showed a high number of defects in absorption with the presence of rGO structures. By virtue of improved optical properties, the rGO-coated glass may be beneficial to be used as a glass coating material for high optical performance of fiber optics.

Keywords: Erbium nanoparticles; rGO; tellurite glass

ABSTRAK

Bahan nano berasaskan grafin mempunyai potensi ketara untuk digunakan sebagai bahan salutan untuk prestasi kaca. Dalam kajian ini, kaca tellurit disalut grafin oksida terkurang (rGO) telah disintesis melalui teknik lebur lindap dan salutan semburan kos rendah untuk meningkatkan sifat optik dalam kaca matriks. Sifat struktur yang dijalankan menggunakan pembelauan sinar-X (XRD) mengesahkan susunan struktur fasa sifat amorfus manakala, analisis mikroskop pengimbasan elektron (SEM) membuktikan imej struktur morfologi rGO pada permukaan kaca tellurit. Nilai indeks biasan kaca disaluti rGO didapati lebih tinggi dalam julat 2.402 - 2.775 disebabkan oleh kesan berasaskan grafin. Nilai tenaga jurang jalur optik kaca disaluti rGO telah meningkat dari 1.913 - 2.980 eV yang dikaitkan dengan perubahan dalam ciri penyerapan rGO. Tenaga Urbach menunjukkan bilangan kekurangan yang tinggi dalam penyerapan dengan kehadiran struktur rGO. Berdasarkan sifat optik yang dipertingkatkan, kaca disaluti rGO bermanfaat untuk digunakan sebagai bahan salutan kaca untuk prestasi tinggi gentian optik.

Kata kunci: Kaca telurit; nanozarah erbium; rGO

INTRODUCTION

Graphene oxide (GO) is oxidized from graphene derivative that possesses an atomic arrangement similar to the graphene sheet due to its oxygenated carbon backbone and adhered mostly with hydroxyl, carboxyl, carbonyl, and epoxide groups on nanosheets (Al-Gaashani et al. 2019). GO has attracted attention as a unique material and solution-possessable multifunction carbon platform via modifying the electronically conducting sp^2 to insulating sp^3 carbon atoms and may tune the bandgap of GO sheets which in turn also affects nonlinear optical (NLO) properties of GO (Abozied et al. 2021; Aradhana et al. 2018). The tuning of bandgap caused by the existence of various oxygen-containing functional groups localized at the edges enables GO as a promising prospect in the field of optoelectronics, sensors, electrodes, as well as lithium-ion batteries (Bhuyan et al. 2016; Cao et al. 2017). However, the higher graphitic structure defects

and hydrophilic nature that existed in GO nanostructures attribute to the weakest optical absorption (Gao et al. 2019). In addition, the role of various functional groups in GO showed weak interactions such as van der Waals forces, electrostatic interactions with negatively-charged surface oxygen functional groups, or π-π interactions with the delocalized π orbitals of graphitic sp^2 carbon domains (Aradhana et al. 2018). Therefore, we introduce a functionally reduced graphene oxide (rGO) as a novel candidate to replace GO in order to tune the optical properties in glass materials by controlling its oxygen content via an electrochemical reduction approach of GO. On reduction, some of the oxygen groups are removed during reduction that allowing the absorption efficiency to be improved, as well as the bandgap energy (Bonavolontà et al. 2021). Hence, we expect that reduced graphene oxide-coated tellurite glass, ZBTEr (NPs)-rGO with the existing layered structure onto the glass surface may improve the optical performance of the glass network system.

Tellurite-based glasses are non-crystalline solids that possess many advantages over conventional borate, phosphate, and silicate glasses, which have been extensively studied for their numerous optical, photonics, and laser applications (Azlan et al. 2019; Umar et al. 2017). Fortunately, tellurite glasses present excellent optical properties which are characterized by having a low melting point, high refractive index (~2.0), high dielectric constant, good chemical stability, wide infrared (IR) transmission range (1-6 μm), and lowest maximum phonon energy (~750 cm^{-1}) among other oxide glasses (Said Mahraz et al. 2013; Wshah et al. 2021; Zhang et al. 2021a, 2021b). All these make the tellurite glass become a promising host material when combined with rGO which may enhance the optical properties of glass materials mainly for fiber optics applications. Rare-earth elements are required for different purposes when doped into glasses, resulting in the possible demand for laser and optical devices (Marzouk, Azooz & El Batal 2021). Thus, it has been identified that Er^{3+} nanoparticles, categorized as the lanthanide oxide nanoparticles significantly may enhance the optical performance of laser glass as reported by Azlan et al. (2019). Additionally, erbium-doped glasses are attractive as may be presented by the upconversion process using near-infrared (NIR) radiation whereby, the transition starts from the excited state ($^4I_{13/2}$) to the ground state ($^4I_{15/2}$) (Liu et al. 2017).

In the present study, the aim was to prepare the tellurite-based glasses coated with rGO by utilizing a simple and low-cost spray coating technique. We first partially reduced GO into rGO using an electrochemical reduction process, and subsequently, the tellurite glass surface was coated with rGO. The morphological structures, refractive index, and optical bandgap energy of the ZBTEr (NPs)-rGO glasses were further investigated. To the best of our knowledge, such an investigation for obtaining highly improved optical properties of ZBTEr(NPs)-rGO glass has not been reported yet. Moreover, this novel study significantly achieves the interesting performance for fiber optics technology as rGO itself would present as a coating material for production in glass coatings.

Materials and Methods

Preparation of RGO

Graphene oxide was synthesized by using an electrochemical exfoliation method. First, two graphite rods were connected to a 5 V static potential of direct current (DC) power supply that has been immersed into an 0.1 M electrolyte solution containing sodium dodecyl sulphate (SDS) surfactant for 24 h exfoliation process. Then, the process of an electrochemical reduction can be explained as the reduction of functional groups existing in GO, which are the epoxide and hydroxyl located on the basal plane of GO which acts as the major components whereas the carbonyl, carboxyl, quinones, lactols, and phenols, are distributed at the edges of GO as the minor components (Sharma et al. 2020). The obtained GO solution was immediately reduced using the hydrazine hydrate as the reducing agent in a triple neck, round bottom flask and ready for immersion process. The mixture was then followed by additional stirring for 24 h at a temperature of ~95 °C.

Fabrication and Deposition of Tellurite-based Glasses

Prior to the preparation of rGO solution via an electrochemical reduction approach as presented above, the tellurite-based glass samples were initially synthesized based on the chemical composition of $(0.47(1-y))\ TeO_2 + (0.2(1-y))\ B_2O_3 + (0.29(1-y))\ ZnO + Er_2O_3(y)$ containing Er_2O_3 nanoparticles with varying molar composition of (y = 0.005, 0.01, 0.02, 0.03, 0.04, and 0.05 mol%). The basic laboratory chemicals were Tellurium (IV) Oxide, TeO_2 (Alfa Aesar, 99.99%), Boron Oxide, B_2O_3 (Alfa Aesar, 98.50%), Zinc Oxide, ZnO (Alfa Aesar, 99.99%), and Erbium (III) Oxide, Er_2O_3 (Alfa Aesar, 99.99%), respectively. The weighed batches were well-mixed in a platinum (Pt) crucible for the pre-heating process at 400 °C for 1 h and subsequently, melted at 900 °C for 2 h. The refined molten was then rapidly quenched into heated a stainless-steel mold based on the

appropriate dimensions. The glass samples were annealed which was regulated at 400 °C for 1 h in order to avoid the mechanical stress. The furnace was switched off and left to cool down overnight at room temperature before being polished to attain a smooth and flat surface. The synthesized glass samples were then coated with rGO by using the low-cost spray coating technique. Finally, the rGO-coated tellurite glass samples were annealed at 400 °C for 1 h and ready for optical and structural characterizations.

SAMPLE CHARACTERIZATION

The rGO solution was coated on the tellurite-based glasses surface via a low-cost spray coating technique. The nozzle of an airbrush system was used for the coating process at approximately ~10 cm constant distance from the nozzle to the glass surfaces. The morphological studies of samples were analyzed using a scanning electron microscope (SEM, Hitachi SU8020) and energy dispersive X-ray (EDX), working at an accelerating voltage of 2 – 30 kV with a magnification range from 1 – 200 K X. A Bruker, D2 Phaser X-ray Diffraction (XRD) operating at Cu-Kα emission (λ = 0.154 nm), using a 2θ angular range from 20° - 90° was performed to prove an amorphous nature of glass samples. Meanwhile, the optical properties of glass samples were characterized via UV-Vis spectroscopy (Agilent Cary 60 Spectrophotometer).

RESULTS AND DISCUSSION

MICROSTRUCTURAL ANALYSIS

The micrographs and morphological observations of the ZBTEr (NPs)-rGO glass surface were investigated via scanning electron microscopy (SEM), as illustrated in Figure 1(a) and 1(b), respectively. The images show the folded regimes and wrinkles due to the large formation of agglomeration rGO structures. Moreover, it can be seen that the appearance of wavy-like structures which indicates the separated graphitic nanosheets during the successful reduction process. Meanwhile, the flakes of rGO are unevenly distributed over the glass surface, as shown in Figure 1(b). This may be correlated to the high percentage of rGO accumulated in a specific region on glass surface due to the uncontrolled spray coating technique thus, resulting in highly dense agglomerated rGO nanostructures. In addition, the presence of very thin and bright layers was observed for ZBTEr (NPs)-

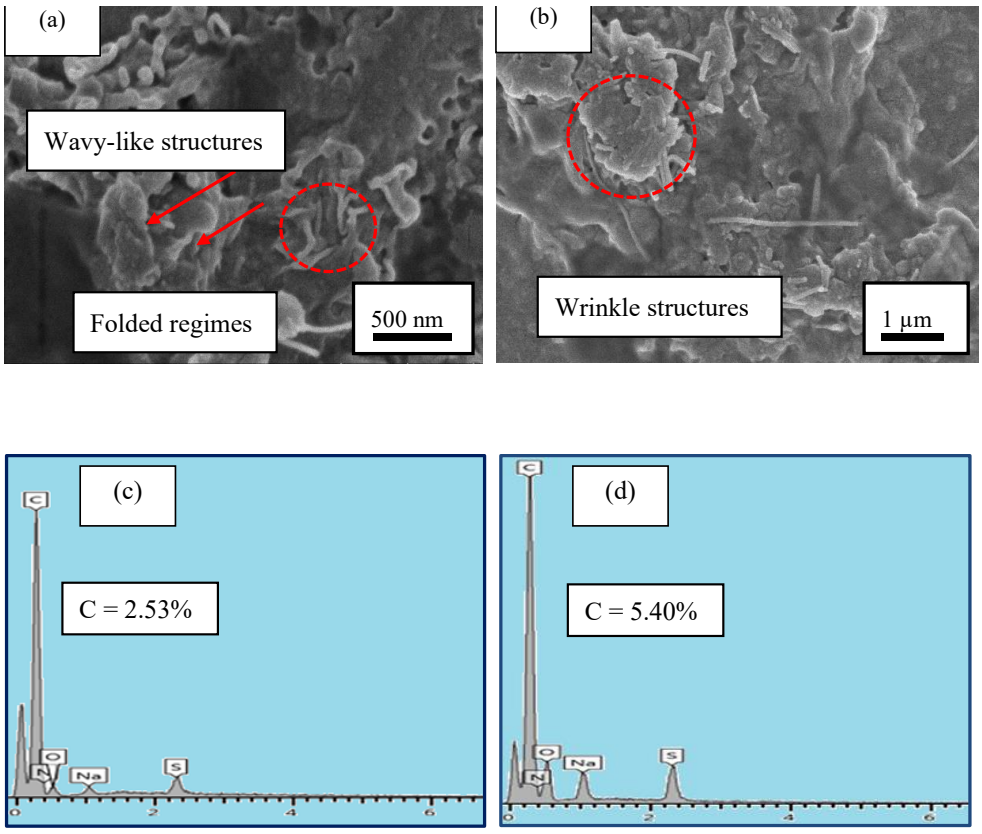

FIGURE 1. Top view images of ZBTEr (NPs)-rGO glass surfaces showing the different rGO structures at 0.03 mol% Er_2O_3 nanoparticles concentration with the magnification of (a) 70 K X, (b) 50 K X, (c) – (d) EDX spectra at the different regions of rGO

rGO glass surface as these characteristics were believed due to the well-dispersed of rGO throughout the electrochemical reduction process and therefore, the rGO layers were seen to be visible and obviously transparent. These findings were supported by EDX analysis which clearly confirmed that rGO was composed of several possible elements including, carbon (C), oxygen (O), sodium (Na), and sulphur (S). It can be noticed from Figure 1(c) and 1(d) that the presence amount of C element exhibited the highest weight percentage estimated at approximately ~2.53% to 5.40% than the other elements.

X-RAY DIFFRACTION (XRD) ANALYSIS

Figure 2 shows the XRD pattern of all prepared rGO-coated tellurite glasses which was recorded in the range of $20° \leq \theta \leq 80°$. The presence of a broad hump between 20° and 30° angle validates the absence of any sharp crystalline diffraction peaks on the diffractogram of ZBTEr (NPs)-rGO glasses. The XRD results also confirm the amorphous in nature as supported by the existence of long-range disorder arrangement of glass materials (Yusof, Ghoshal & Azlan 2017).

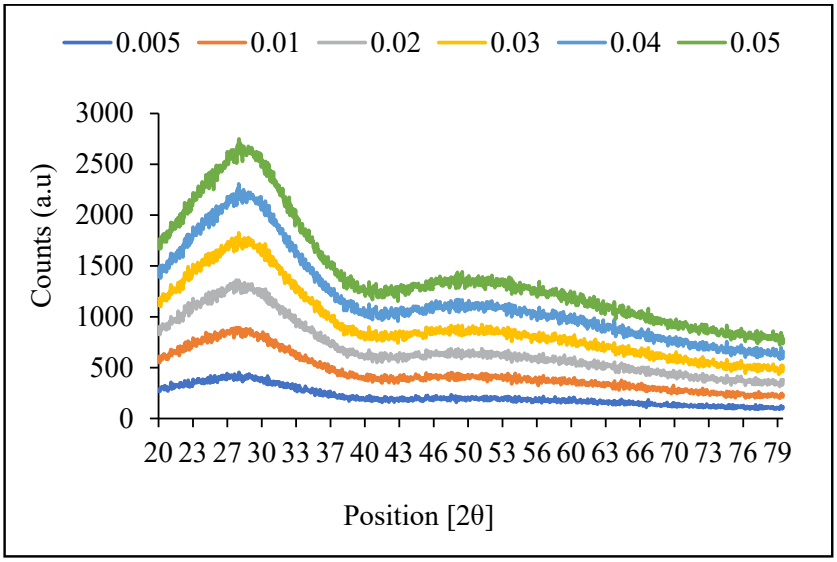

FIGURE 2. XRD pattern of ZBTEr(NPs)-rGO glasses

OPTICAL BANDGAP AND URBACH ENERGY

Ultraviolet-visible (UV-Vis) spectroscopy is the vital analysis to investigate the nature of glasses by identifying the optical properties such as the optical absorption, optical bandgap, and Urbach energy (Effendy et al. 2021). The fundamental optical bandgap may be correlated with the valence and conduction bands whereby the electrons move freely from the valence to the conduction bands in order to allow the electrical conductivity in the material. The optical bandgap of glass samples can be determined from the absorbance spectra, which firstly calculate the optical absorption coefficient, α(ω) by the following relation:

$$\alpha(\omega)=2.303\left(\frac{A}{d}\right) \quad (1)$$

where A and d are denoted as the absorbance and thickness of glass samples, respectively.

According to Mott and Davis's theory, the relation between absorption coefficient, α(ω), and photon energy, Ħω was utilized to determine the optical bandgap energy in glass materials as given herewith (Mott, Davis & Weiser 1972):

$$\alpha(\omega)=\frac{\beta(\hbar\omega-Eopt)^{n}}{\hbar\omega} \quad (2)$$

where β is a constant called the band tailing parameter; E_{opt} is the optical bandgap; and n represents the constant index which refers to the optical transitions.

The optical bandgap of glass samples was estimated from Tauc's plot, a graph plotting of $(\hbar\omega)$ vs $(\alpha\hbar\omega)$ which extrapolates the linear portion to the x-axis and gives the value of bandgap (E_{opt}), as shown in Figure 3. The calculated optical bandgap value for

ZBTEr (NPs)-rGO glasses were found to be in the range between 1.913 and 2.980 eV which is decreased compared to the ZBTEr (NPs) glasses, as presented in Figure 4 and tabulated in Table 1, respectively. It could be observed that the deposition of rGO onto the glass surface alters the bandgap energy of ZBTEr (NPs)-rGO glasses which may be due to the absorption transitions in C=O (*n*-π) and C=C (π-π*) states present in the graphitic material, respectively (Sreeja et al. 2017). Moreover, the improvement in optical absorption is due to the increased amount of sp^2 hybridized carbon atoms in rGO whereby, the oxygen contents are partly removed during the reduction process. The glass coating reveals the strong bonding interaction between the rGO and tellurite-based glass surfaces and thus, decreasing the optical bandgap.

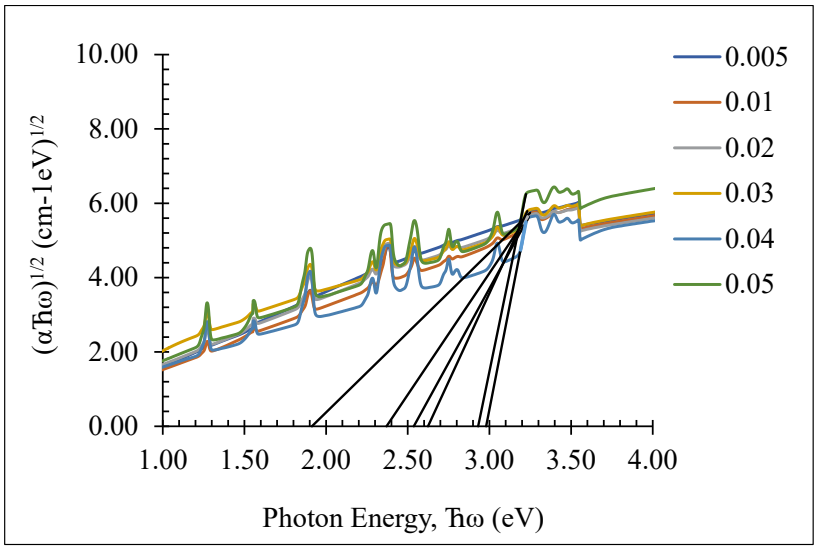

FIGURE 3. Tauc's plot of $(\alpha\hbar\omega)^{1/2}$ against photon energy, $\hbar\omega$ of ZBTEr (NPs)-rGO glasses

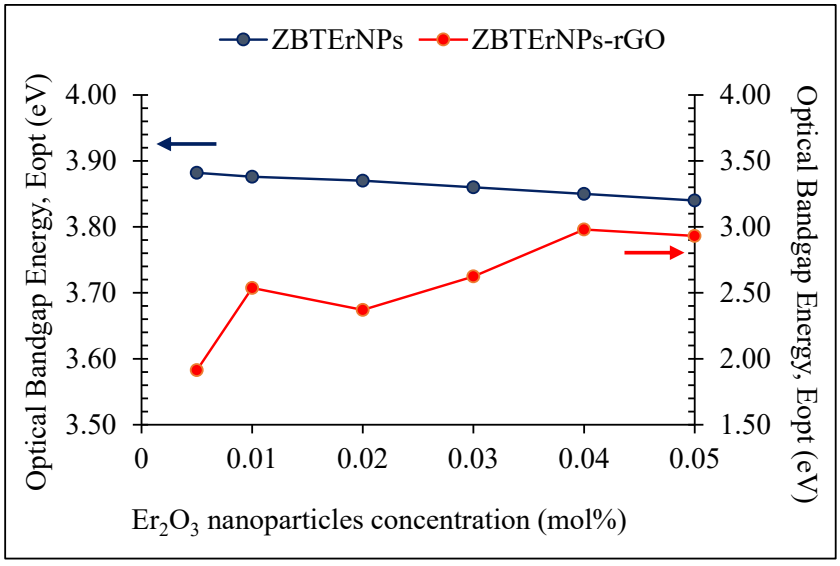

FIGURE 4. Variation of optical bandgap values for ZBTEr (NPs) and ZBTEr (NPs)-rGO glasses

TABLE 1. Comparison of optical bandgap energy (E_{opt}) between ZBTEr (NPs) and ZBTEr (NPs)-rGO glasses

Er_2O_3 nanoparticles concentration (mol%)	Optical bandgap energy, Eopt (eV) ZBTEr (NPs) (Azlan et al. 2015)	Optical bandgap energy, E_{opt} (eV) ZBTEr (NPs)-rGO
0.005	3.882 ± 0.1	1.913 ± 0.1
0.01	3.876 ± 0.1	2.537 ± 0.1
0.02	3.870 ± 0.1	2.370 ± 0.1
0.03	3.860 ± 0.1	2.624 ± 0.1
0.04	3.850 ± 0.1	2.980 ± 0.1
0.05	3.840 ± 0.1	2.931 ± 0.1

Urbach energy, ΔE is a parameter typically relates to the degree of structural disorder in amorphous materials which converts the weak bonds into defects (Tiwari & Dhondiyal 2021). The degree of disorderliness occurred in amorphous materials due to the additional broadening and thus, could attribute to the tailing of energy states in the forbidden gap (Shakeri & Rezvani 2011). Consequently, the Urbach energy values can be determined by taking the reciprocals of the slopes of the linear portion based on the plotted graph between log (α) and photon energy ($\hbar\omega$) curves. The Urbach energy can be expressed as:

$$\alpha(\omega) = \beta \exp\left(\frac{\hbar\omega}{\Delta E}\right) \quad (3)$$

This exponential behavior gives the increase in band tail states associated with the valence and conduction bands which caused the reduction in optical bandgap energy (Dimitrov & Sakka 1996; Sreeja & Anila 2019). Figure 5 and Table 2 present the variation of Urbach energy values of ZBTEr (NPs)-rGO glasses which was found in the range of 0.118 to 0.408 eV. In this work, the increasing trend in Urbach energy values from 0.005 to 0.02 mol% indicates the higher number of defects in the glass network or an increase in non-bridging oxygen (Amjad et al. 2013). Meanwhile, the Urbach energy values were seen to gradually decrease by increasing the Er_2O_3 nanoparticles content attributed to the decrease in broadening of static disorder-related parts (El-Diasty,

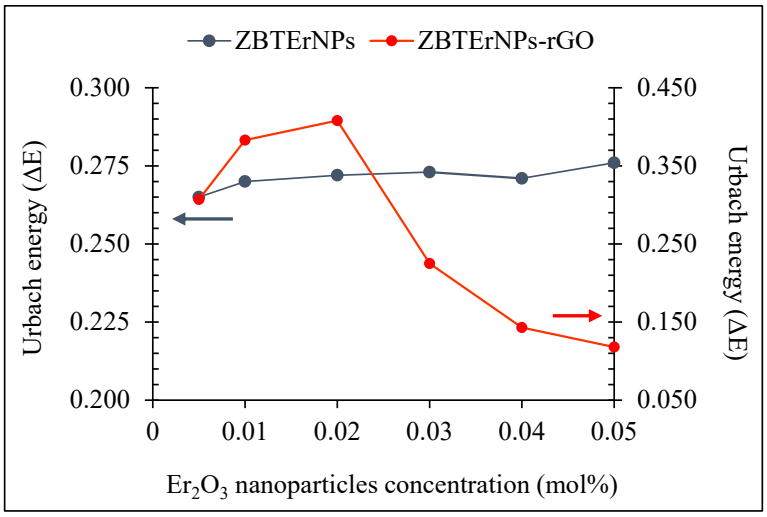

FIGURE 5. Variation of Urbach energy values for ZBTEr (NPs) and ZBTEr (NPs)-rGO glasses

Wahab & Abdel-Baki 2006). This trend can also be correlated with the low level of oxygen atoms and the formation of agglomerated structures that appeared on the glass surface that caused the lower defects compared to the ZBTEr (NPs) glasses. In addition, these results are clearly proved by the morphological analysis, as demonstrated in Figure 1.

TABLE 2. Comparison of Urbach energy (ΔE) between ZBTEr (NPs) and ZBTEr (NPs)-rGO glasses

Er_2O_3 nanoparticles concentration (mol%)	Urbach energy, ΔE (eV) ZBTEr (NPs) (Azlan et al. 2015)	Urbach energy, ΔE (eV) ZBTEr (NPs)-rGO
0.005	0.265 ± 0.1	0.307 ± 0.1
0.01	0.270 ± 0.1	0.383 ± 0.1
0.02	0.272 ± 0.1	0.408 ± 0.1
0.03	0.273 ± 0.1	0.225 ± 0.1
0.04	0.271 ± 0.1	0.143 ± 0.1
0.05	0.276 ± 0.1	0.118 ± 0.1

REFRACTIVE INDEX

The refractive index is an important measurement that may affect the candela distribution of the transmitted light and easy to change the intensity of light by improving the refractive index value of the material (Tiwari & Dhondiyal 2021). Theoretically, the fundamental of refractive index can be estimated using the optical bandgap energy (Dimitrov & Sakka 1996) and thus, can be written as:

$$\frac{n^2-1}{n^2+1} = 1\text{-}\sqrt{\frac{E_{opt}}{20}} \quad (4)$$

where n is the refractive index and E_{opt} represents optical bandgap energy.

It can be observed from the plotted graph that the refractive index value of ZBTEr (NPs)-rGO glasses exhibit an increasing trend in the range of 2.402 to 2.775 compared to ZBTEr (NPs) glass, as shown in Figure 6 and tabulated in Table 3. This trend can be correlated to

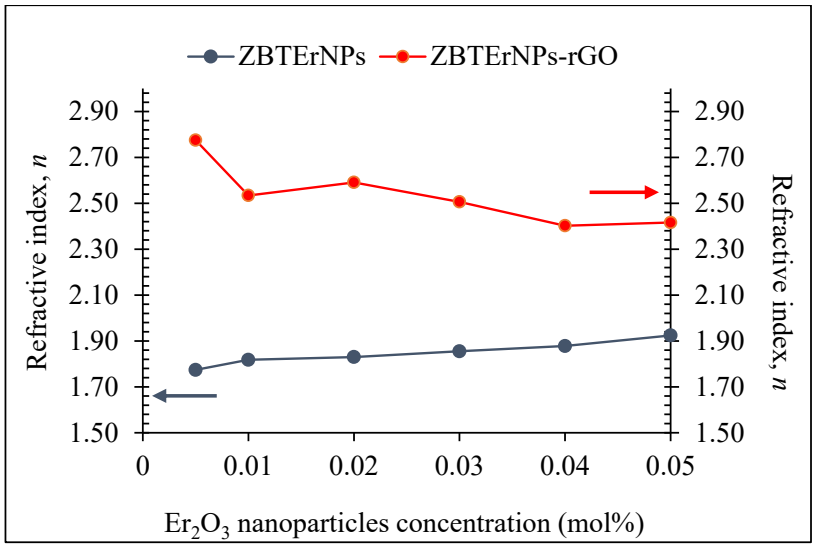

FIGURE 6. Variation of refractive index values for ZBTEr (NPs) and ZBTEr (NPs)-rGO glasses

the high number of sp^2 carbon atoms and redistribution of delocalized π-electrons resulting from the removal of the oxygen functional groups in rGO nanosheets which attributes as the main component of optical nonlinearity in this glass material (Omidvar et al. 2018). On the other hand, the enhanced value in the refractive index of ZBTEr (NPs)-rGO glass confirms the formation of localized energy levels form between the conduction and valence bands and may create the free carriers belonging to the sp^2 electron domain in rGO structures (Jiménez-pérez et al. 2018). Therefore, the result significantly shows the great performance of graphene-coated glass material whereby, the refractive index values achieve the condition under the refractive index of fiber core must be slightly higher than that of cladding.

TABLE 3. Comparison of refractive index (*n*) values between ZBTEr (NPs) and ZBTEr (NPs)-rGO glasses

Er_2O_3 nanoparticles concentration (mol%)	Refractive index, n ZBTEr (NPs) (Azlan et al. 2015)	Refractive index, *n* ZBTEr (NPs)-rGO
0.005	1.774 ± 0.1	2.775 ± 0.1
0.01	1.818 ± 0.1	2.534 ± 0.1
0.02	1.830 ± 0.1	2.591 ± 0.1
0.03	1.855 ± 0.1	2.506 ± 0.1
0.04	1.878 ± 0.1	2.402 ± 0.1
0.05	1.924 ± 0.1	2.416 ± 0.1

CONCLUSION

In summary, the optical properties of ZBTEr (NPs)-rGO glasses have been successfully studied. The optical bandgap energy of ZBTEr (NPs)-rGO glasses decreased than ZBTEr (NPs) glasses. It is noticed that low oxygen content in rGO coating onto glass surfaces improves the optical properties of glass samples. The XRD analysis validated that the ZBTEr (NPs) glasses are amorphous in nature. The SEM images proved the existence of rGO structures on the glass surface. The decreasing value in optical bandgap energy of ZBTEr (NPs)-rGO glasses was due to the changes in optical absorption characteristics. The Urbach energy value presented the high defects after being coated with rGO. The refractive index of ZBTEr (NPs)-rGO glasses also demonstrated a high value than ZBTEr (NPs) glasses which can be related to the bonding between delocalized π-electrons and lower oxygen content existed in rGO layers.

ACKNOWLEDGEMENTS

This research was financially supported by Skim Geran Penyelidikan Fundamental (FRGS) Fasa 1/2018 (Grant code: 2019-0006-102-02). The authors would like to thank the following institutions for equipment support: Faculty of Science and Mathematics, Universiti Pendidikan Sultan Idris and Faculty of Science, Universiti Putra Malaysia.

REFERENCES

Abozied, A.M., Mostafa, A.M., Abouelsayed, A., Hassan, A.F., Ramadan, A.A., Al-Ashkar, E.A. & Anis, B. 2021. Preparation, characterization, and nonlinear optical properties of graphene oxide thin film doped with low chirality metallic SWCNTs. *Journal of Materials Research and Technology* 12: 1461-1472.

Al-Gaashani, R., Najjar, A., Zakaria, Y., Mansour, S. & Atieh, M.A. 2019. XPS and structural studies of high quality graphene oxide and reduced graphene oxide prepared by different chemical oxidation methods. *Ceramics International* 45: 14439-14448.

Amjad, R.J., Sahar, M.R., Ghoshal, S.K., Dousti, M.R. & Arifin, R. 2013. Synthesis and characterization of Dy^{3+} doped zin –lead-phosphate glass. *Optical Materials* 35: 1103-1108.

Aradhana, D.M., Dissanayake, S., Cifuentes, M.P. & Humphrey, M.G. 2018. Optical limiting properties of (reduced) graphene oxide covalently functionalized by coordination complexes. *Coordination Chemistry Reviews* 375: 489-513.

Azlan, M.N., Halimah, M.K., Suriani, A.B., Azlina, Y., Umar, S.A. & El-Mallawany, R. 2019. Upconversion properties of erbium nanoparticles doped tellurite glasses for high efficient laser glass. *Optics Communications* 448: 82-88.

Azlan, M.N., Halimah, M.K., Shafinas, S.Z. & Daud, W.M. 2015. Electronic polarizability of zinc borotellurite glass system containing erbium nanoparticles. *Materials Express* 5(3): 211-218.

Bhuyan, M.S.A., Uddin, M.N., Islam, M.M., Bipasha, F.A. & Hossain, S.S. 2016. Synthesis of graphene. *International Nano Letters* 6(2): 65-83.

Bonavolontà, C., Vettoliere, A., Falco, G., Aramo, C., Rendina, I., Ruggiero, B., Silvestrini, P. & Valentino, M. 2021. Reduced graphene oxide on silicon-based structure as novel broadband photodetector. *Scientific Reports* 11: 13015.

Cao, Y., Chai, D., Luo, Z., Jiang, M., Xu, W., Xiong, C., Li, S., Liu, H. & Fang, D. 2017. Lithium vanadate nanowires@ reduced graphene oxide nanocomposites on titanium foil with super high capacities for lithium-ion batteries. *Journal of Colloid and Interface Science* 498: 210-216.

Dimitrov, V. & Sakka, S. 1996. Linear and nonlinear optical properties of simple oxides. II. *Journal of Applied Physics* 79(3): 1741-1745.

Effendy, N., Sidek, H.A.A., Halimah, M.K. & Zaid, M.H.M. 2021. Enhancement on thermal, elastic and optical properties of new formulation tellurite glasses: Influence of ZnO as a glass modifier. *Materials Chemistry and Physics* 273: 125156.

El-Diasty, F., Wahab, F.A.A. & Abdel-Baki, M. 2006. Optical band gap studies on lithium aluminum silicate glasses doped with Cr^{3+} ions. *Journal of Applied Physics* 100: 093511.

Gao, X., Ju, P., Liu, X., Chen, L., Ji, L., Li, H., Zhou, H. & Chen, J. 2019. Macro-tribological behaviors of four common graphenes. *Industrial and Engineering Chemistry Research* 58(14): 5464-5471.

Jiménez-Pérez, J.L., Gutiérrez-Fuentes, R., López-Gamboa, G. & Sánchez-Ramírez, J.F. 2018. Measurement of optical nonlinear refractive index response of graphene nanoparticles dispersed in an aqueous solution by Z scan technique. *Optical Materials* 84: 236-241.

Liu, D., Li, C., Xu, Y., Zhou, D., Wang, H., Sun, P. & Jiang, H. 2017. Near-infrared luminescent erbium complexes with 8-hydroxyquinoline-terminated hyperbranched polyester. *Polymer* 113: 274-282.

Marzouk, S.Y., Azooz, M.A. & El Batal, H.A. 2021. Judd-Ofelt analysis of spectroscopic measurements of Er^{3+} doped boro-zincate glasses. *Journal of Molecular Structure* 1243: 130925.

Mott, N.F., Davis, E.A. & Weiser, K. 1972. Electronic processes in non-crystalline materials. *Physics Today* 25(12): 55.

Omidvar, A., RashidianVaziri, M.R. & Jaleh, B. 2018. Enhancing the nonlinear optical properties of graphene oxide by repairing with palladium nanoparticles. *Physica E: Low-Dimensional Systems and Nanostructures* 103: 239-245.

Said Mahraz, Z.A., Sahar, M.R., Ghoshal, S.K. & Reza Dousti, M. 2013. Concentration dependent luminescence quenching of Er^{3+}-doped zinc boro-tellurite glass. *Journal of Luminescence* 144: 139-145.

Shakeri, M.S. & Rezvani, M. 2011. Optical band gap and spectroscopic study of lithium alumino silicate glass containing Y^{3+} ions. *Spectrochimica Acta Part A: Molecular and Biomolecular Spectroscopy* 79: 1920-1925.

Sharma, N., Arif, M., Monga, S., Shkir, M., Mishra, Y.K. & Singh, A. 2020. Investigation of bandgap alteration in graphene oxide with different reduction routes. *Applied Surface Science* 513: 145396.

Sreeja, V.G. & Anila, E.I. 2019. Studies on the effect of reduced graphene oxide on nonlinear absorption and optical limiting properties of potassium doped zinc oxide thin film by Z - scan technique. *Thin Solid Films* 685: 161-167.

Sreeja, V.G., Vinitha, G., Reshmi, R., Anila, E.I. & Jayaraj, M.K. 2017. Effect of reduction time on third order optical nonlinearity of reduced graphene oxide. *Optical Materials* 66: 460-468.

Tiwari, H. & Dhondiyal, C.C. 2021. Physical and optical analysis of Sm^{3+} doped zinc phosphate glass. *Materials Today: Proceedings* 47(Part 8): 1682-1688.

Umar, S.A., Halimah, M.K., Chan, K.T. & Latif, A.A. 2017. Polarizability, optical basicity and electric susceptibility of Er^{3+} doped silicate borotellurite glasses. *Journal of Non-Crystalline Solids* 471: 101-109.

Wshah, A.A.A., Halimah, M.K., Alazoumi, S.H., Umar, S.A. & Ibrahim, G.G. 2021. Elastic properties of TeO_2–ZnO–Ag_2O doped with Nd_2O_3. *Materials Chemistry and Physics* 260: 124195.

Yusof, N.N., Ghoshal, S.K. & Azlan, M.N. 2017. Optical properties of titania nanoparticles embedded Er^{3+}-doped tellurite glass: Judd-Ofelt analysis. *Journal of Alloys and Compounds* 724: 1083-1092.

Zhang, Y., Xia, L., Li, C., Ding, J., Li, J. & Zhou, Y. 2021a. Enhanced 2.7 μm mid-infrared emission in Er^{3+}/Ho^{3+} co-doped tellurite glass. *Optics and Laser Technology* 138: 106913.

Zhang, Y., Xia, L., Shen, X., Li, J., Yang, G. & Zhou, Y. 2021b. Broadband mid-infrared emission in Dy^{3+}/Er^{3+} co-doped tellurite glass. *Journal of Luminescence* 236: 118078.

*Corresponding author; email: azlanmn@fsmt.upsi.edu.my